The Effect of the Dielectric Layer Thickness on Spectral Performance of CdZnTe Frisch Collar Gamma Ray Spectrometers

Alireza Kargar, *Member, IEEE*, Adam C. Brooks, Mark J. Harrison, *Member, IEEE*, Kyle T. Kohman, Rans B. Lowell, Roger C. Keyes, Henry Chen, Glenn Bindley, and Douglas S. McGregor, *Member, IEEE*

***Abstract*—The spectral performance as a function of the dielectric layer thickness for several CdZnTe Frisch collar devices was investigated. Seven different planar bar shaped detectors were fabricated from Redlen Technologies CdZnTe, and many Frisch collar devices were prepared from each planar device. The optimum dielectric layer thickness was experimentally determined for each device. The result of the optimal thickness study was verified through three-dimensional geometry modeling of the potential and electric field. It is shown that there exists an optimal dielectric layer thickness for best performance for CdZnTe Frisch collar devices with aspect ratios (L/W) greater than 2.5.**

***Index Terms*—CdZnTe Frisch collar detector, dielectric thickness.**

I. Introduction

CdZnTe Frisch collar devices have shown promise for numerous applications, such as medical imaging, astrophysics isotope identification, and remote gamma ray spectroscopy. The Frisch collar detector consists of a block of semiconductor material with opposing contacts at two ends of the block. A dielectric insulating layer is coated around the bar, followed by a conductive coating. In past work, Teflon tape was used as the insulator and Cu shim was used as the conductive coating [1]–[3]. The Cu shim can be connected to one of the contacts, or it may be connected to a separate potential, including ground. Details of the device configuration are described elsewhere [1], [4], [5].

The thickness of the dielectric layer between the bare CdZnTe semiconductor crystal and the conductive collar has been reported to impact the device performance significantly [6]. Different methods of applying the dielectric and collar were also investigated [6]. Further, the effect of device geometry on the spectral performance of Frisch collar detectors was previously reported [7]. However, the limitations on the aspect ratio (AR, length L over width W) of the bar shaped Frisch collar detectors were determined only for thin layers of dielectric [7]. In this study, the optimal thicknesses of the dielectric layer for a few specific Frisch collar device geometries were experimentally determined. These results are verified through modeling of the weighting potential and electric field of the desired device. Teflon tape was used as the dielectric layer to fabricate CdZnTe Frisch collar devices.

As the dielectric layer thickness of the two-terminal Frisch collar device increases, the overall device AR decreases. A decrease in AR affects the nonlinearity of the weighting potential distribution by forcing it towards a linear distribution. Unfortunately, this change degrades the device performance, especially if the aspect ratio of the device is significantly altered [7]. Similarly, the great difference in permittivity κ of CdZnTe ($\kappa_1 = 11$) and the dielectric layer ($\kappa_2 \approx 2$ for Teflon) also forces the weighting potential towards a linear distribution as the dielectric thickness increases. Yet, the *operating* potential profile also moves towards a linear distribution, thereby increasing the electric field near the cathode region, which can potentially improve the device performance by improving charge carrier transport. Hence, increasing the dielectric thickness has two different effects on device performance in which one effect improves device performance (operating potential or electric field), and the other deteriorates device performance (weighting potential).

A *nonlinear* weighting potential is best for a single carrier device, which works to accent the influence on induced charge for one charge carrier type over the other (for instance, electrons over holes), thereby improving energy resolution [1]. Yet, for two terminal devices, the operating potential mimics the shape of the weighting potential, hence produces a low electric field region near the cathode. A *linear* operating potential results in a better electric field distribution throughout the device and reduced electron trapping in the region near the cathode of the device. Therefore, there is an optimum dielectric layer thickness for a given crystal geometry, set of charge transport properties, applied bias and permittivity of the dielectric layer.

II. Theoretical Considerations

Based on Green's Reciprocation Theorem [8]–[10], if the series of charges $Q_1, Q_2, \ldots, Q_n$ on a system of conductors produce potentials of $V_1, V_2, \ldots, V_n$ on each of the conductors respectively (initial condition); and likewise, another series of charges $Q'_1, Q'_2, \ldots, Q'_n$ on the same system of conductors

Manuscript received June 30, 2008; revised September 16, 2008. Current version published June 10, 2009. This work was supported in part by the U.S. Department of Energy under NEER Grant DE-FG07-03ID14498, by DTRA contract DTRA-01-02-D-0067, and by NNSA through Brookhaven National Laboratories subcontract 126181.

A. Kargar, A. C. Brooks, M. J. Harrison, K. T. Kohman, R. B. Lowell, R. C. Keyes, and D. S. McGregor are with the S.M.A.R.T. Laboratory, Kansas State University, Manhattan, KS 66506 USA (e-mail: kargar@ksu.edu).

H. Chen and G. Bindley are with Redlen Technologies, Sidney, BC V8L 5Y8, Canada.

Color versions of one or more of the figures in this paper are available online at http://ieeexplore.ieee.org.

Digital Object Identifier 10.1109/TNS.2009.2017193

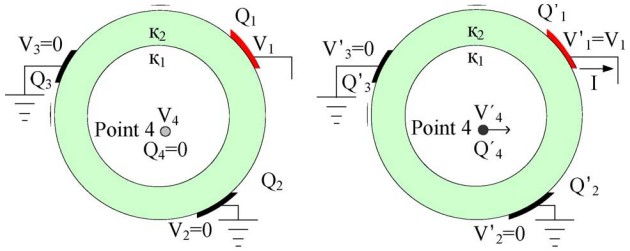

Fig. 1. The Shockley-Ramo theorem [9], [10] for three electrodes resembling a two-terminal Frisch collar device. Two of the electrodes are held at zero potential or grounded, while the collecting electrode senses the generation and motion of the excited charge as a result of a radiation interaction.

give potentials of $V'_1, V'_2, \ldots, V'_n$ respectively (final condition), then

$$\sum_{i=1}^{n} Q_i V'_i = \sum_{i=1}^{n} Q'_i V_i \tag{1}$$

is valid for this system of conductors. Now, assume that four points in space are labeled 1 through 4, with points 1 through 3 stationed on three conductors, as shown in Fig. 1. A finite number of dielectric layers with specific values of permittivity exist between conductors (two dielectric layers are shown Fig. 1 with different permittivity of κ_1 and κ_2). Point 4 is an arbitrary point where the numerical value of potential is trivial. Applying (1) for the system shown in Fig. 1,

$$Q_1 V'_1 = Q'_1 V_1 + Q'_4 V_4.$$

Considering the fact that $V_1 = V'_1$, then

$$Q_1 - Q'_1 = Q'_4 \left(\frac{V_4}{V_1}\right). \tag{2}$$

The term $(Q_1 - Q'_1)$ is termed the induced charge ΔQ_1, which can be sensed on conductor 1 by a charge sensitive preamplifier. It should be noted that this amount of charge ΔQ_1 is first induced as a result of generation of charge Q'_4 at point 4 (such as a radiation interaction). As Q'_4 moves in space to a new point, it continues inducing charge on the conductor 1 in the same manner explained. The derivative of induced charge ΔQ_1 with respect to time is the induced current I. The term (V_4/V_1) is called weighting potential ψ [11], where obviously $0 \leq \psi \leq 1$. It should be noted that V_4 is the potential at point 4 which can be calculated with appropriate boundary conditions ($V_2 = V_3 = 0$, V_1), arrangement of conductors, and the permittivities of the materials. It is obvious that no space charge exists for the initial condition as shown in Fig. 1.

In most cases, in order to estimate the induce charge, it would be simpler to solve Laplace's equation (no space charge ρ) for the weighting potential ψ,

$$\nabla (\kappa \varepsilon_0 \nabla \psi) = 0 \tag{3}$$

TABLE I
THE PLANAR AND FRISCH COLLAR DEVICES NAME AND DIMENSIONS

Planar Device Name	Planar Device Dimension (mm)	Number of Fabricated Frisch Collar Devices	Frisch Collar Device Names	AR[a]
Device 1	4.95x4.76 L=4.87	4	Device 1 #1 to #4	1.0
Device 2	4.70x4.56 L=6.03	4	Device 2 #1 to #4	1.3
Device 3	3.36x3.34 L=5.68	6	Device 3 #1 to #6	1.7
Device 4	3.96x4.01 L=11.60	13	Device 4 #1 to #13	2.9
Device 5	3.92x3.89 L=10.82	11	Device 5 #1 to #11	2.8
Device 6	5.01x4.73 L=19.63	7	Device 6 #1 to #7	4.0
Device 7	5.00x4.70 L=19.60	14	Device 7 #1 to #14	4.0

[a]AR is the average aspect ratio (device length L over device average width W) of the planar devices.

with the boundary condition of $\psi = 1$ at the collecting electrode and $\psi = 0$ for all other electrodes considering the permittivities of the materials. For the potential V, Poisson's equation must be solved

$$\nabla (\kappa \varepsilon_0 \nabla V) = -\rho \tag{4}$$

with all the electrodes at their appropriate potential, considering the permittivities of the materials and the space charges. However, it is generally assumed that space charges are negligible in CdZnTe, hence ρ is small and Poisson's equation is simplified to Laplace's equation. With this assumption, the weighting potential distribution ψ and the normalized operating potential distribution are identical for a two-terminal Frisch collar device.

III. EXPERIMENTAL PROCEDURES AND SETUPS

A. Device Designs and Preparation

In order to investigate the effect of dielectric thickness on the performance of Frisch collar CdZnTe devices, seven planar devices in a variety of sizes were fabricated. Raw CdZnTe materials were acquired from Redlen Technologies and fabricated into Frisch collar devices with different dielectric layer thicknesses. The planar devices were labeled as Device 1 through Device 7. The size of the planar devices and the names of the subsequently fabricated Frisch collar devices are listed in Table I.

Both planar and Frisch collar devices were prepared in the manner previously reported in [2]. Teflon tape was used as the dielectric layer in fabricating the Frisch collar devices. The dimensions of each Teflon wrapped device were measured using a micrometer to evaluate the thickness of the dielectric layer. Once the dielectric layer was applied, the conductive copper shim was cut to size and used as the Frisch collar. The conductive collar covered the entire lateral surface of the device and was connected to the device cathode. As each Frisch collar device was prepared, a spectral performance measurement was conducted. The conductive collar was then removed to fabricate the next Frisch collar device by either adding or removing Teflon

TABLE II
THE PLANAR AND FRISCH COLLAR DEVICES EXPERIMENTAL SETUPS

Planar Device Name	Preamplifier and connector	Amplifier Gain	Bias (V)	Device to Source Distance (mm)	Real Time (s)
Device 1	ORTEC 142A - BNC	100X	736	23.6±0.1	3600
Device 2	ORTEC 142A - BNC	100X	905	23.6±0.1	3600
Device 3	ORTEC 142A - BNC	100X	1000	23.6±0.1	3600
Device 4	CANBERRA 2001A - SHV	50X	1600	20.8±0.1	1800
Device 5	CANBERRA 2001A - SHV	50X	1500	20.8±0.1	1800
Device 6	CANBERRA 2001A - SHV	10X	3000	0.0 [a]	900
Device 7	CANBERRA 2001A - SHV	50X	2400	20.8±0.1	1800

[a]A different standard ^{137}Cs gamma ray source was used for Device 6, while only this device was placed directly on the source.

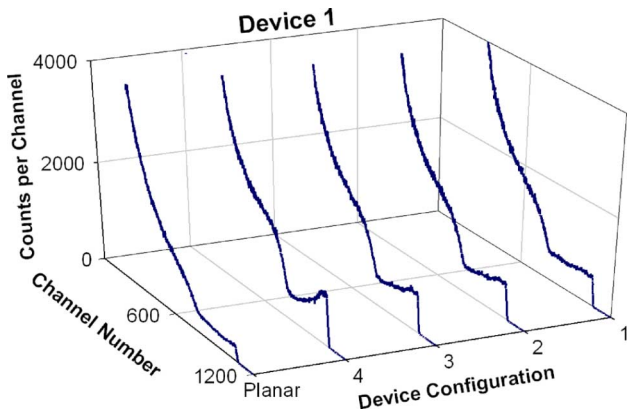

Fig. 2. The pulse height spectra of Device 1 (4.95×4.76 mm^2 $\times$ L $=$ 4.87 mm) taken with standard gamma ray source of ^{137}Cs. The applied bias, amplifier gain and the spectral testing time are presented in Table II. The dielectric thickness t is presented in Table III for Frisch collar Device 1 #1 to Device 1 #4. The best spectral performance is for Device 1 #4 which has the thinnest dielectric layer ($t = 0.05$ mm).

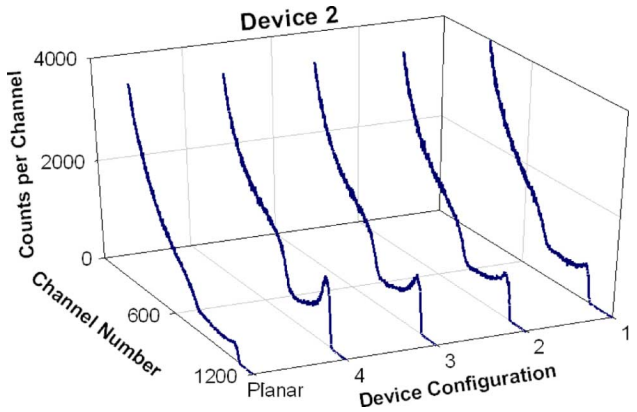

Fig. 3. The pulse height spectra of Device 2 (4.70×4.56 mm^2 $\times$ L $=$ 6.03 mm) taken with a standard ^{137}Cs gamma ray sources. The applied bias, amplifier gain and the spectral testing time are presented in Table II. The dielectric thickness t is presented in Table III for Frisch collar Device 2 #1 to Device 2 #4. The best spectral performance is for Device 2 #4, which has the thinnest dielectric layer ($t = 0.05$ mm).

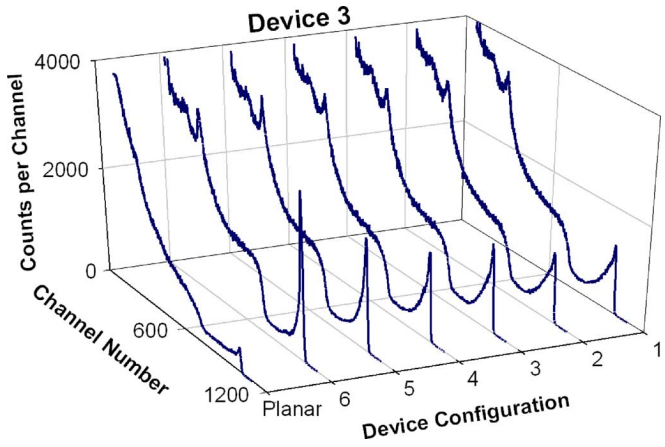

Fig. 4. The pulse height spectra of Device 3 (3.36×3.34 mm^2 $\times$ L $=$ 5.68 mm) taken with a standard ^{137}Cs gamma ray source. The applied bias, amplifier gain and the spectral testing time are presented in Table II. The dielectric thickness t is presented in Table III for Frisch collar Device 3 #1 to Device 3 #6. The best spectral performance is for Device 3 #6, which has the thinnest dielectric layer ($t = 0.10$ mm). Device 3 #6 shows $2.1\% \pm 0.1\%$ FWHM energy resolution at 662 keV.

layer(s). Finally, a new conductive copper shim was added to complete the new Frisch collar device.

B. Device Testing

Two measurements were taken with each device: a ^{137}Cs pulse height spectrum and a current-voltage (I-V) curve. The I-V curve measurement was performed only for the planar devices, while a ^{137}Cs spectrum was recorded for every device in planar and all Frisch collar configurations. The details are provided in the following sections.

1) The Spectral Measurement: The pulse height spectra were acquired for devices in both planar and Frisch collar configurations using standard ^{137}Cs calibration sources. The CdZnTe detectors were mounted in aluminum test boxes such that the detector cathode faced the gamma ray source. The gamma ray source was placed outside the project box, except for Device 6, in which the source was placed directly underneath the detector. The aluminum test box was then connected to a preamplifier with an appropriate connector (see Table II). The aluminum test box and the preamplifier were then placed inside a copper Faraday cage to minimize electronic noise. The preamplifier was connected to a high-voltage supply, amplifier (CANBERRA Model 2021), and a pulse generator. An oscilloscope, a multichannel analyzer (MCA), and a personal computer were used to monitor and acquire the data.

The temperature and the relative humidity were recorded to be 23 ± 2°C and $50 \pm 5\%$, respectively for all experiments. An amplifier shaping time of 1 μs was held constant for all spectra collected. However, the amplifier gain, the operating bias and the device to source distance were different. These settings are presented in Table II for all the spectral measurements. The bias was held constant for each device when operated either as planar or Frisch collar devices. Data collection time also varied for

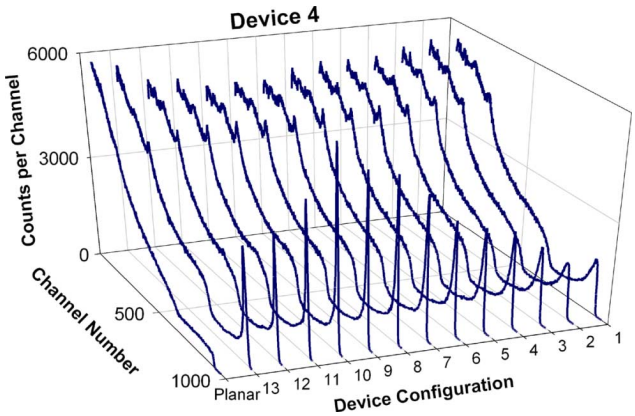

Fig. 5. The pulse height spectra of Device 4 ($3.96 \times 4.01\ \mathrm{mm}^2 \times \mathrm{L} = 11.60\ \mathrm{mm}$) taken with standard ^{137}Cs gamma ray sources. The applied bias, amplifier gain and the spectral testing time are presented in Table II. The dielectric thickness t, the energy resolution and the peak-to-valley are presented in Table IV for Frisch collar Device 4 #1 to Device 4 #13. The best spectral performance is for Device 4 #10, which has the optimum dielectric layer thickness of $t_{opt} = 0.27\ \mathrm{mm}$. Device 4 #10 shows $1.4\% \pm 0.1\%$ FWHM energy resolution at 662 keV.

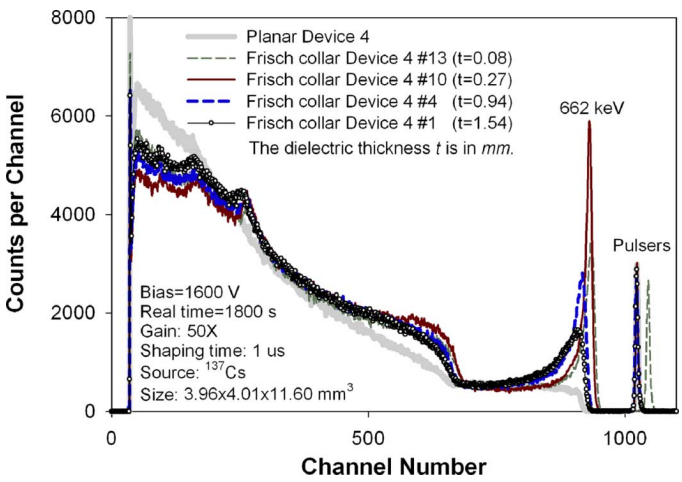

Fig. 6. The pulse height spectra of Device 4 taken with a standard ^{137}Cs gamma ray source. The best spectral performance is for Device 4 #10, which has the optimum dielectric layer thickness of $t_{opt} = 0.27\ \mathrm{mm}$. Device 4 #10 shows $1.4\% \pm 0.1\%$ FWHM energy resolution at 662 keV and peak-to-valley of 13.9 ± 0.5.

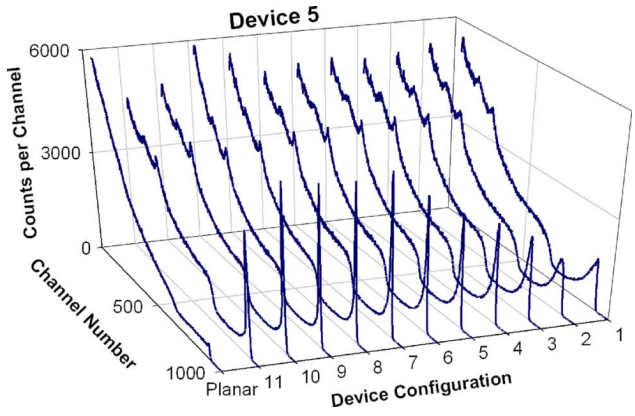

Fig. 7. The pulse height spectra of Device 5 ($3.92 \times 3.89\ \mathrm{mm}^2 \times \mathrm{L} = 10.82\ \mathrm{mm}$) taken with a standard ^{137}Cs gamma ray source. The applied bias, amplifier gain and the spectral testing time are presented in Table II. The dielectric thickness t, the energy resolution and the peak-to-valley are presented in Table IV for Frisch collar Device 5 #1 to Device 5 #11. The best spectral performance is for Device 5 #8, which has the optimum dielectric layer thickness of $t_{opt} = 0.39\ \mathrm{mm}$. Device 5 #8 shows $1.3\% \pm 0.1\%$ FWHM energy resolution at 662 keV.

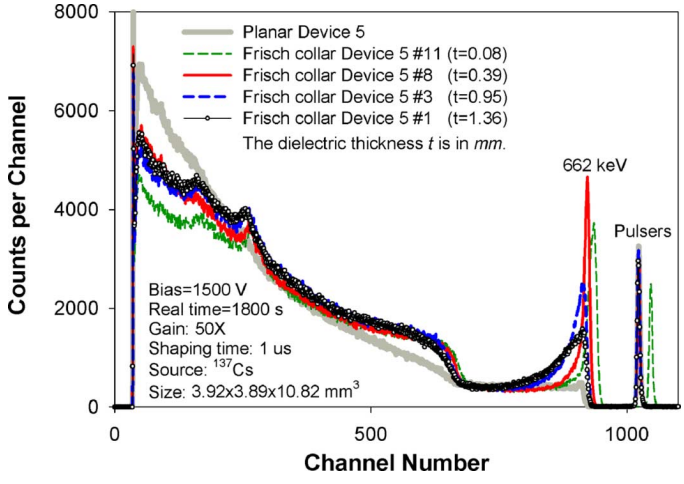

Fig. 8. The pulse height spectra of Device 5, taken with a standard ^{137}Cs gamma ray source, for specific dielectric thicknesses. The best spectral performance is for Device 5 #8, which has the optimum dielectric layer thickness of $t_{opt} = 0.39\ \mathrm{mm}$. Device 5 #8 shows $1.3\% \pm 0.1\%$ FWHM energy resolution at 662 keV and peak-to-valley of 14.3 ± 0.7.

different detectors, which are recorded in Table II. However, the collection time was the same for each device in both planar and all Frisch collar configurations as mentioned in Table II.

2) The Current-Voltage Characteristic Measurement: A Keithley I-V Curve Tracer was used to perform the I-V curve measurements. The voltage increment was set to 5.0 V while the delay at each voltage point was set to 0.5 seconds. The maximum/minimum regulated voltage was set to ± 1000 V.

IV. Results

Figs. 2–12 display the energy spectra for the devices listed in Tables I and II in both planar and Frisch collar configurations with standard ^{137}Cs gamma ray sources. Figs. 2–4 show the energy spectra for Device 1 to Device 3, respectively. The results show device improvement for the thinnest dielectric layer for Device 1 to Device 3. It should be noted that for Device 1 and Device 2, there is not a great enhancement as a result of the Frisch collar effect, even with a thin dielectric layer. This is due to fact that the aspect ratio of the planar devices are smaller than 1.5, and do not meet the minimum aspect ratio as reported previously [7]. The dielectric layer thicknesses for Device 1 to Device 3 in Frisch collar configurations are also summarized in Table III.

Figs. 5–8 presents the energy spectra for Device 4 and Device 5, in both planar and Frisch collar configuration with standard gamma ray sources of ^{137}Cs. The results indicate an optimum dielectric layer thickness t_{opt} for which both Device 4 and Device 5 reach their best spectral performance. The optimum dielectric layer thickness t_{opt} for Device 4 is around 0.27 mm and for Device 5 is around 0.39 mm. The dielectric layer thicknesses for Device 4 and Device 5 in Frisch collar configurations, the full

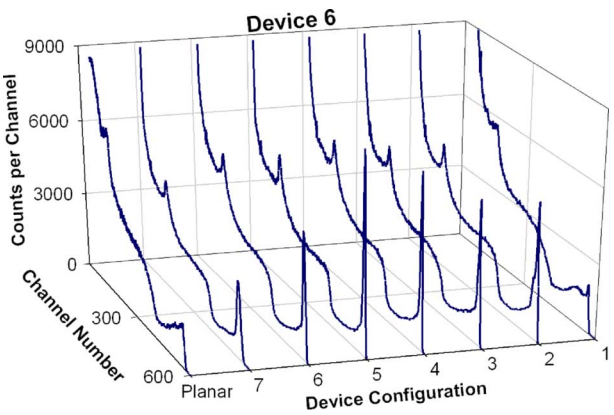

Fig. 9. The pulse height spectra of Device 6 ($5.01 \times 4.73\ \mathrm{mm}^2 \times \mathrm{L} = 19.63\ \mathrm{mm}$) taken with a standard ^{137}Cs gamma ray source. The applied bias, amplifier gain and the spectral testing time are presented in Table II. The dielectric thickness t, the energy resolution and the peak-to-valley are presented in Table V for Frisch collar Device 6 #1 to Device 6 #7. The best spectral performance is for Device 6 #5, which has the optimum dielectric layer thickness of $t_{opt} = 1.10\ \mathrm{mm}$. Device 6 #5 shows $1.6\% \pm 0.2\%$ FWHM energy resolution at 662 keV.

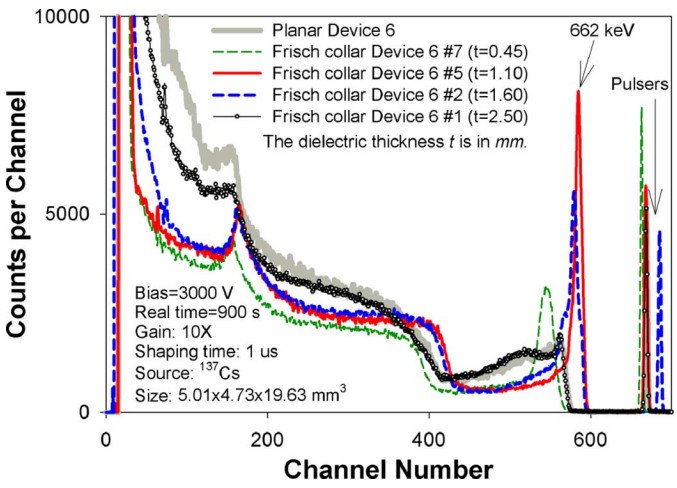

Fig. 10. The pulse height spectra of Device 6, taken with a standard ^{137}Cs gamma ray source, for specific dielectric thicknesses. The best spectral performance is for Device 6 #5, which has the optimum dielectric layer thickness of $t_{opt} = 1.10\ \mathrm{mm}$. Device 6 #5 shows $1.6\% \pm 0.2\%$ FWHM energy resolution at 662 keV and peak-to-valley of 15.1 ± 0.4.

width half maximum (FWHM) energy resolution at 662 keV and the peak-to-valley ratio (P:V) of the full energy peak (FEP) are also summarized in Table IV.

A similar effect occurs for Device 6 and Device 7, as shown in Figs. 9–12 showing the energy spectra with standard ^{137}Cs gamma ray sources. The optimum dielectric layer thickness t_{opt} for Device 6 is around 1.10 mm and for Device 7 is around 0.70 mm. The summary of the dielectric layer thicknesses for Device 6 and Device 7 in Frisch collar configurations, the FWHM energy resolution at 662 keV and the P:V of the FEP are listed in Table V. The current-voltage (IV) characteristics

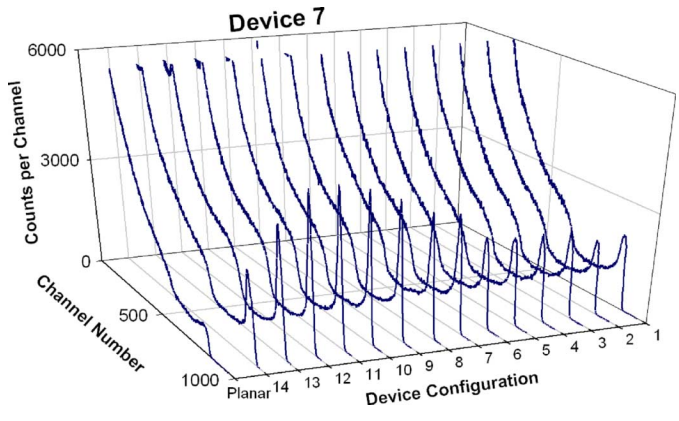

Fig. 11. The pulse height spectra of Device 7 ($5.00 \times 4.70\ \mathrm{mm}^2 \times \mathrm{L} = 19.60\ \mathrm{mm}$) taken with a standard ^{137}Cs gamma ray source. The applied bias, amplifier gain and the spectral testing time are presented in Table II. The dielectric thickness t, the energy resolution and the peak-to-valley are presented in Table V for Frisch collar Device 7 #1 to Device 7 #14. The best spectral performance is for Device 7 #10, which has the optimum dielectric layer thickness of $t_{opt} = 0.70\ \mathrm{mm}$. Device 7 #10 shows $2.4\% \pm 0.1\%$ FWHM energy resolution at 662 keV.

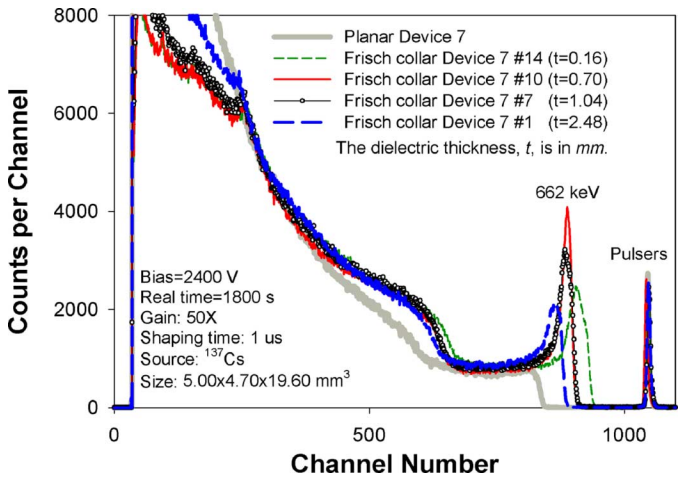

Fig. 12. The pulse height spectra of Device 7, taken with a standard ^{137}Cs gamma ray source, for specific dielectric thicknesses. The best spectral performance is for Device 7 #10, which has the optimum dielectric layer thickness of $t_{opt} = 0.70\ \mathrm{mm}$. Device 7 #10 shows $2.4\% \pm 0.1\%$ FWHM energy resolution at 662 keV and peak-to-valley of 5.9 ± 0.12.

TABLE III
SUMMARY OF DIELECTRIC LAYER THICKNESSES FOR DEVICE 1 TO DEVICE 3

Frisch collar Device Name	Dielectric Thickness, t (mm)		
	Device 1	Device 2	Device 3
1	0.27	0.27	0.38
2	0.16	0.16	0.32
3	0.10	0.10	0.27
4	0.05	0.05	0.22
5	N/A	N/A	0.16
6	N/A	N/A	0.10

TABLE IV
SUMMARY OF ENERGY RESOLUTION AND PEAK-TO-VALLEY FOR DIFFERENT DIELECTRIC LAYER THICKNESSES OF DEVICE 4 AND DEVICE 5

Frisch collar Device Name	Device 4			Device 5		
	t [a]	%R [b]	P:V [c]	t [a]	%R [b]	P:V [c]
1	1.54	N/A	3.0±0.1	1.36	N/A	4.0±0.2
2	1.34	4.6%	3.0±0.1	1.16	4.9%	4.1±0.2
3	1.14	3.8%	4.2±0.1	0.95	3.4%	7.0±0.3
4	0.94	3.0%	5.1±0.1	0.81	2.6%	8.5±0.4
5	0.80	2.8%	6.7±0.2	0.70	2.0%	8.4±0.3
6	0.70	2.5%	6.9±0.2	0.60	1.7%	10.7±0.4
7	0.59	2.0%	8.3±0.2	0.50	1.5%	13.0±0.5
8 [d]	0.5	1.9%	10.9±0.4	**0.39**	**1.3%**	**14.3±0.7**
9	0.38	1.7%	11.2±0.4	0.27	1.4%	14.1±0.6
10 [e]	**0.27**	**1.4%**	**13.9±0.5**	0.16	1.7%	12.1±0.4
11	0.22	1.7%	10.7±0.4	0.08	2.0%	10.1±0.4
12	0.16	1.9%	7.8±0.2	N/A	N/A	N/A
13	0.08	2.2%	7.2±0.2	N/A	N/A	N/A

[a]The dielectric thickness t is in *mm* with the standard deviation of ±0.005 mm.
[b]%R is the full width half maximum (FWHM) energy resolution in % at 662 keV with the standard deviation of ±0.1%.
[c]P:V is the peak-to-valley ratio of the full energy peak (FEP).
[d]The best performance of Device 5 was for Frisch collar Device 5 #8 with the optimum dielectric thickness t_{opt} of 0.39 mm.
[e]The best performance of Device 4 was for Frisch collar Device 4 #10 with the optimum dielectric thickness t_{opt} of 0.27 mm.

TABLE V
SUMMARY OF ENERGY RESOLUTION AND PEAK-TO-VALLEY FOR DIFFERENT DIELECTRIC LAYER THICKNESSES OF DEVICE 6 AND DEVICE 7

Frisch collar Device Name	Device 6			Device 7		
	t [a]	%R [b]	P:V [c]	t [a]	%R [b]	P:V [c]
1	2.50	N/A	2.2±0.1	2.48	N/A	2.3±0.04
2	1.60	3.5%	10.5±0.3	2.15	N/A	2.4±0.04
3	1.40	1.6%	9.1±0.2	1.90	3.5%	2.7±0.05
4	1.25	1.6%	11.0±0.3	1.70	3.5%	3.0±0.05
5 [d]	**1.10**	**1.6%**	**15.1±0.4**	1.62	3.5%	3.1±0.05
6	0.95	2.2%	8.4±0.2	1.52	3.5%	2.9±0.05
7	0.45	4.0%	5.5±0.1	1.04	3.0%	4.1±0.07
8	N/A	N/A	N/A	0.87	2.9%	3.9±0.07
9	N/A	N/A	N/A	0.75	2.6%	5.2±0.10
10 [e]	N/A	N/A	N/A	**0.70**	**2.4%**	**5.9±0.12**
11	N/A	N/A	N/A	0.66	2.9%	6.1±0.13
12	N/A	N/A	N/A	0.51	3.4%	6.1±0.13
13	N/A	N/A	N/A	0.37	4.0%	5.2±0.11
14	N/A	N/A	N/A	0.16	4.7%	2.7±0.05

[a]The dielectric thickness t is in *mm* with the standard deviation of ±0.005 mm.
[b]%R is the full width half maximum (FWHM) energy resolution in % at 662 keV with the standard deviation of ±0.1%.
[c]P:V is the peak-to-valley ratio of the full energy peak (FEP).
[d]The best performance of Device 6 was for Frisch collar Device 6 #5 with the optimum dielectric thickness t_{opt} of 1.10 mm.
[e]The best performance of Device 7 was for Frisch collar Device 7 #10 with the optimum dielectric thickness t_{opt} of 0.70 mm.

curves obtained for planar devices listed in Table II are presented in Fig. 13.

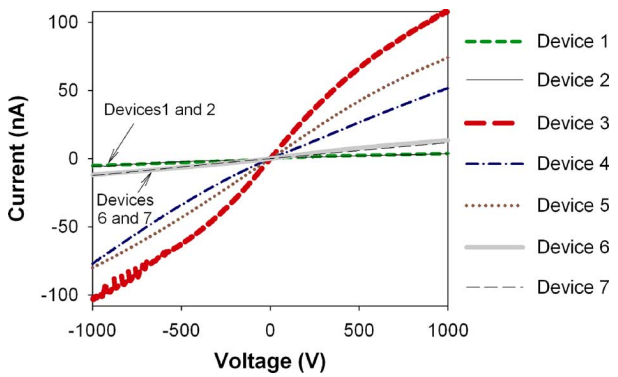

Fig. 13. The current-voltage (IV) characteristics curve of all devices in planar configurations.

V. DISCUSSIONS

It can be determined from the experimental results of the seven Frisch collar devices tested that, for those devices with the aspect ratio greater than 2.5 (Device 4 to Device 7), there appears to be an optimum dielectric thickness for best performance. For the Frisch collar devices with aspect ratios smaller than 2.0, the thinnest possible dielectric thickness appears to perform better, however, the dielectric layer should be thick enough to stop extra leakage current from the conductive collar to the anode. Therefore, the main role of the dielectric layer in Frisch collar devices with $\mathrm{AR} < 2$ is to prevent extra leakage current between the conductive collar and the anode.

For the Frisch collar devices with $\mathrm{AR} > 2.5$ (Device 4 to Device 7) and very thin dielectric layers $\approx 0.10\,\mathrm{mm}$ (thick enough to stop the leakage current), the relatively low performance of the device is due to low electric field region in a large portion of the device. This low electric field region results in electron trapping which degrades the device performance. This effect becomes more important for Frisch collar devices with $\mathrm{AR} > 3$ (Frisch collar Device 6 #7 and Device 7 #14). The effect can be predicted by modeling the weighting/operating potential and the electric field for a specific device and configuration. The Frisch collar devices, in this study, were modeled in three-dimensional geometry, and the weighting/operating potential and electric field distributions were determined using Integrated Engineering Software, LORENTZ. The weighting/operating potential and electric field distribution along the device central axis for Device 4 and Device 7 are presented in Figs. 14–17. For very thin dielectric layer, more than half of the volume of Frisch collar Device 4 suffers from extremely low electric field (close to zero as shown in Fig. 15). The very low electric field region occurs in two-thirds of Frisch collar Device 7 (and Device 6) with very thin dielectric layer. The abovementioned explanation gives reasons for the low performance of Frisch collar Device 6 #7 and Device 7 #14 (Figs. 9–12).

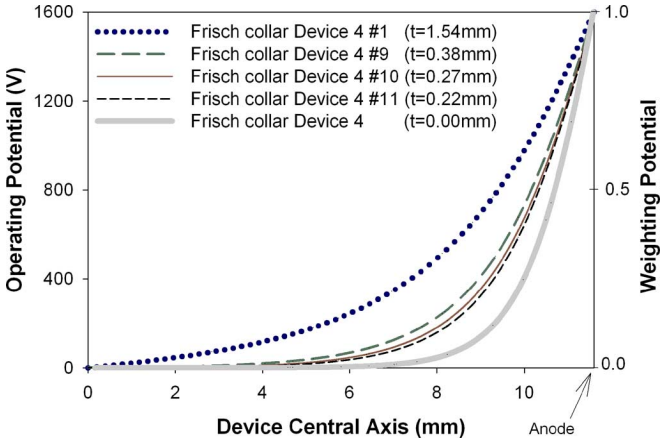

Fig. 14. The operating and weighting potential distributions for Device 4 in Frisch collar configurations along the central axis. The plot shows the potential distributions for the maximum and minimum dielectric thickness t, and in the vicinity of the optimum dielectric thickness t_{opt}, where the Frisch collar Device 4 #10 shows the best performance.

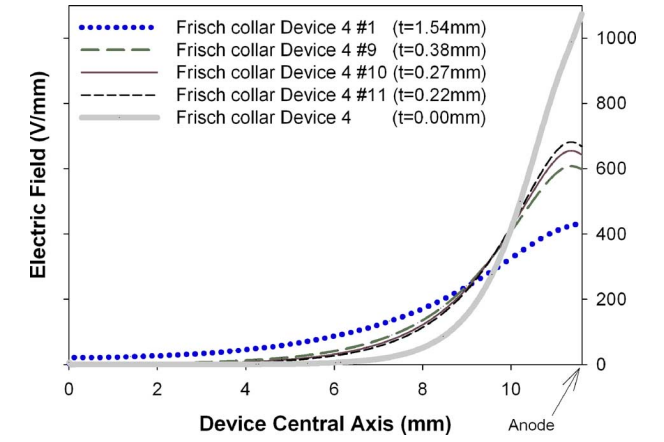

Fig. 15. The electric field distribution for Device 4 in Frisch collar configurations along the central axis. The plot shows the electric field distribution for the maximum and minimum dielectric thickness t, and in the vicinity of the optimum dielectric thickness t_{opt}, where the Frisch collar Device 4 #10 shows the best performance.

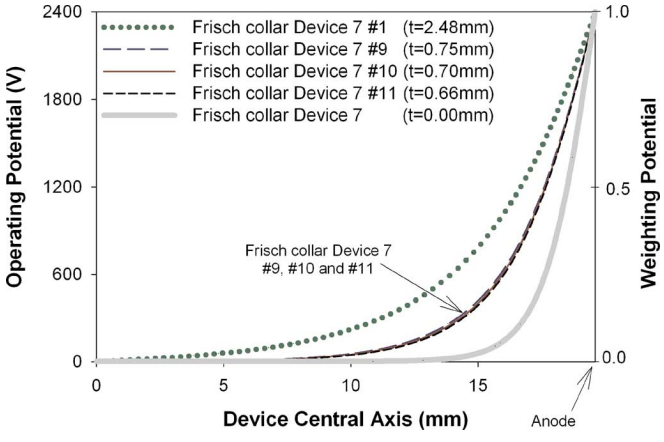

Fig. 16. The operating and weighting potential distributions for Device 7 in Frisch collar configurations along the central axis. The plot shows the potential distributions for the maximum and minimum dielectric thickness t, and in the vicinity of the optimum dielectric thickness t_{opt}, where the Frisch collar Device 7 #10 shows the best performance.

As the dielectric layer thickness of the Frisch collar device increases, a more uniform electric field distribution is achieved

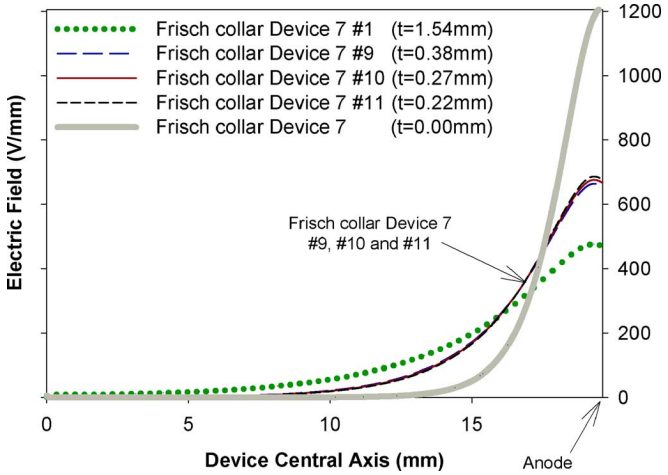

Fig. 17. The electric field distribution for Device 7 in Frisch collar configurations along the central axis. The plot shows the electric field distribution for the maximum and minimum dielectric thickness t, and in the vicinity of the optimum dielectric thickness t_{opt}, where the Frisch collar Device 7 #10 shows the best performance.

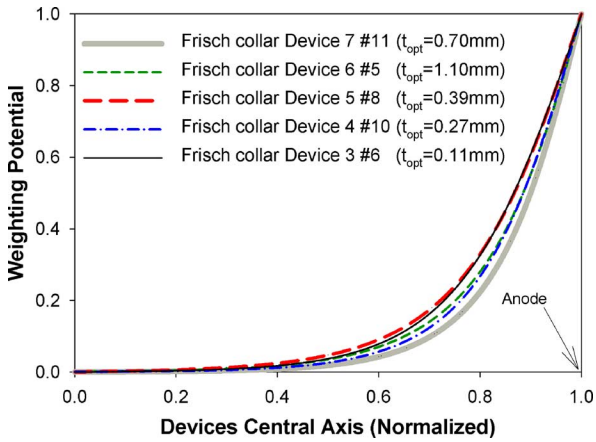

Fig. 18. The weighting potential distributions for Device 3, Device 4, Device 5, Device 6 and Device 7 in Frisch collar configurations along the normalized central axis. The plot shows the weighting potential distributions for the optimum dielectric thickness t_{opt}, where the Frisch collar devices show the best performance. The graph shows a region of optimum distribution for weighting potentials for all Frisch collar devices with a normalized length, which falls between Frisch collar Device 5#8 (upper limit) and Device 7#11 (lower limit).

(Figs. 15 and 17); but, the weighting potential distribution becomes more linear (Figs. 14 and 16). The more linear weighting potential distribution, which approaches the weighting potential of a planar device, reduces the single carrier charge induction effect for electrons. Hence, the device no longer performs as a single carrier device (Device 1 #1 through Device 7 #1).

A Frisch collar device of $\mathrm{AR} > 2.5$, with too thin or thick of a dielectric layer, has compromised spectral performance. Hence, the challenge is to determine the optimum dielectric layer thickness t_{opt}, for such a Frisch collar device. Fig. 18 shows the weighting potential distribution along the device normalized length of Frisch collar Device 3 to Device 7 for their best performance (optimum dielectric layer thickness t_{opt}). Obviously, there is an optimum region of best performance for weighting potential distribution (or normalized operating potential in two-terminal device). In this optimum region, there is

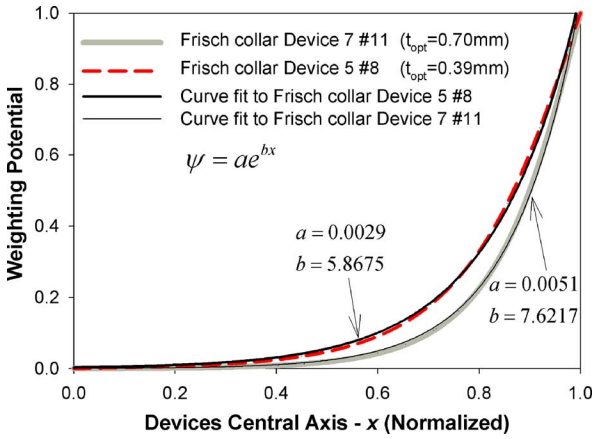

Fig. 19. The weighting potential distributions ψ for Device 5 and Device 7 in Frisch collar configurations along the normalized central axis x with an exponential curve fit to the plots. ψ is the weighting potential, and x and is the normalized central axis ($0 \leq \psi$ and $x \leq 1$). The curves are fit through 'least squares fitting' method.

a balance between improved induced charge (more *nonlinear* weighting potential distribution) and a more uniform electric field (more *linear* operating potential distribution). In Fig. 19, this optimum region of weighting potential distribution is identified by its boundaries with an exponential function fit to those boundary distributions for four Frisch collar devices showing decent performance.

VI. Conclusion and Future Work

In this study the optimum dielectric layer thickness was experimentally determined for several two-terminal bar shape CdZnTe Frisch collar gamma ray spectrometers. An optimum region for the weighting potential (or normalized operating potential) distribution along the normalized device length was determined for the optimum dielectric layer thickness. It is believed that for a two-terminal Frisch collar device, the weighting potential distribution needs to fall in this optimum region (Fig. 19). For the bar shape CdZnTe devices with aspect ratio (AR) greater than 2.5, this optimum region of potential distribution was experimentally determined by changing the dielectric layer thickness. However, reaching the optimum region can be achieved by shortening the conductive collar length; or a combination of both dielectric thickness and conductive collar length. These techniques allow the potential distribution to become more linear and fall in the optimum region, enhancing the electric field distribution. For Frisch collar devices with AR less than 1.5, neither the thicker dielectric nor the shorter conductive length produces appreciable changes to improve performance. Therefore, the only other option is to take advantage of both Frisch collar and small pixel effect, and make the Frisch collar device with the anode to cathode area smaller than unity.

In order to further investigate the optimum region, different conductive length and different dielectric materials need to be studied in the future, especially for high aspect ratio Frisch collar devices. Collimated gamma ray probing along the device length for the Frisch collar devices with $\mathrm{AR} > 3$ and a thin dielectric layer needs to be performed for charge collection characterization. Finally, since the improvement of the two-terminal Frisch collar device performance is due to electric field enhancement, a three-terminal [12] (or four-terminal) Frisch collar device needs to be tested in a similar manner to determine optimum configurations. For this type of multi-terminal device, the weighting potential and the normalized operating potential are no longer the same and they are decoupled, which can potentially improve the device charge collection efficiency.

References

[1] W. J. McNeil, D. S. McGregor, A. E. Bolotnikov, G. W. Wright, and R. B. James, "Single charge carrier type sensing with an insulated Frisch ring CdZnTe semiconductor radiation detector," *Appl. Phys. Lett.*, vol. 84, pp. 1988–1990, 2004.

[2] A. Kargar, A. M. Jones, W. J. McNeil, M. J. Harrison, and D. S. McGregor, "CdZnTe Frisch collar detectors for γ-ray spectroscopy," *Nucl. Instrum. Methods*, vol. A558, pp. 497–503, 2006.

[3] A. Kargar, A. M. Jones, W. J. McNeil, M. J. Harrison, and D. S. McGregor, "Angular response of a W-collimated room-temperature-operated CdZnTe Frisch collar spectrometer," *Nucl. Instrum. Methods*, vol. A562, pp. 262–271, 2006.

[4] D. S. McGregor and R. A. Rojeski, "High Resolution Ionization Detectors and Array of Such Detectors," U.S. Patent US-6175120, Jan. 16, 2001.

[5] D. S. McGregor, "Collimated Radiation Detector Assembly, Array of Collimated Radiation Detectors and Collimated Radiation Detector Module," U.S. Patent US-6781132, Aug. 24, 2004.

[6] M. J. Harrison, A. Kargar, A. C. Brooks, and D. S. McGregor, "Improved techniques for the fabrication of Frisch collar CdZnTe gamma ray spectrometers," in *IEEE Nuclear Science Symp.*, Waikiki, Hawaii, Oct.-Nov. 28–3, 2007.

[7] A. Kargar, R. B. Lowell, M. J. Harrison, and D. S. McGregor, "The crystal geometry and the aspect ratio effects on spectral performance of CdZnTe Frisch collar device," *Proc. SPIE*, vol. 6706, pp. 1J1–1J17, 2007.

[8] W. R. Smythe, *Static and Dynamic Electricity*, 3rd. ed. New York: McGraw-Hill, 1968.

[9] W. Shockley, "Currents to conductors induced by a moving point charge," *J. Appl. Phys.*, vol. 9, pp. 635–636, 1938.

[10] S. Ramo, "Currents induced by electron motion," *Proc. IRE*, pp. 584–585, Sep. 1939.

[11] V. Radeka, "Low-noise techniques in detectors," *Ann. Rev. Nucl. Part. Sci.*, vol. 38, pp. 217–277, 1988.

[12] D. S. McGregor, Z. He, H. A. Seifert, D. K. Wehe, and R. A. Rojeski, "Single charge carrier type sensing with a parallel strip pseudo-Frisch-grid CdZnTe semiconductor radiation detector," *Appl. Phys. Lett.*, vol. 72, pp. 792–794, 1998.